Journal of Hazardous Materials 448 (2023) 130876

Contents lists available at ScienceDirect

Journal of Hazardous Materials

journal homepage: www.elsevier.com/locate/jhazmat

Research Paper

Chemicals of emerging concern in coastal aquifers: Assessment along the land-ocean interface

Daniel Gutiérrez-Martín [a], Rubén Gil-Solsona [a,*], Maarten W. Saaltink [b,c], Valentí Rodellas [d], Rebeca López-Serna [e,f], Albert Folch [b,c], Jesús Carrera [a,b], Pablo Gago-Ferrero [a,*]

[a] Institute of Environmental Assessment and Water Research (IDAEA), CSIC, Jordi Girona 18, 08034 Barcelona, Spain
[b] Associated Unit: Hydrogeology Group (UPC-CSIC), Spain Department of Civil and Environment, Spain
[c] Department of Civil and Environmental Engineering (DECA), Universitat Politècnica de Catalunya (UPC), Jordi Girona 1-3, 08034 Barcelona, Spain
[d] Institut de Ciència i Tecnologia Ambiental, Universitat Autònoma de Barcelona, Bellaterra, Spain
[e] Department of Analytical Chemistry, Faculty of Sciences, University of Valladolid, 47011 Valladolid, Spain
[f] Institute of Sustainable Processes, Dr. Mergelina s/n, Valladolid 47011, Spain

HIGHLIGHTS

- Submarine groundwater discharge was evaluated as a source of sea contamination.
- 92 chemicals of emerging concern (CECs) were detected in coastal aquifer.
- Unique spatial characterization of the CECs present in the land-ocean interface.
- 6 PFAS and 2 pharmaceuticals revealed to be tracers of contamination in groundwater.
- A PFAS, non-previously detected in environmental waters, was tentatively identified.

GRAPHICAL ABSTRACT

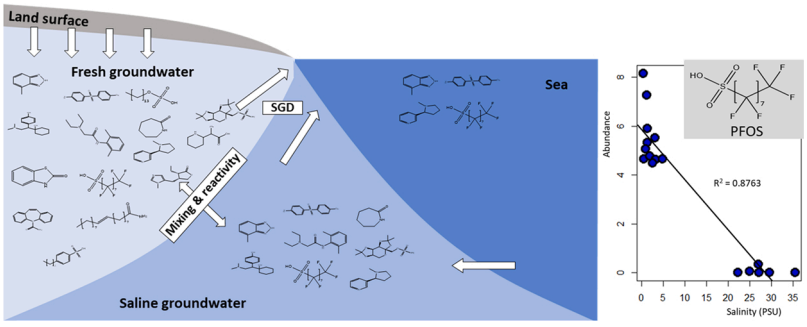

ARTICLE INFO

Editor: Lee Blaney

Keywords:
Coastal aquifer
Submarine groundwater discharge (SGD)
Emerging pollutants
Non-target analysis
High-resolution mass spectrometry (HRMS)
Perfluoroalkyl and polyfluoroalkyl substances (PFAS)

ABSTRACT

Submarine Groundwater Discharge (SGD) is recognized as a relevant source of pollutants to the sea, but little is known about its relevance as a source of chemicals of emerging concern (CECs). Here, both the presence and distribution of a wide range of CECs have been evaluated in the most comprehensive manner to date, in a well-characterized Mediterranean coastal aquifer near Barcelona (Spain). Samples from coastal groundwater and seawater allowed for the unique spatial characterization of the pollutants present in the land-ocean interface, an outstanding research gap that required attention. The main goals were (1) to determine CECs in the aquifer, so as to evaluate the SGD as a relevant source of marine pollution, and (2) to identify new tracers to improve our understanding of SGD dynamics. To this end, 92 CECs were located in the aquifer by using wide-scope analytical target methodologies (>2000 chemicals). Among them, the perfluoroalkyl and polyfluoroalkyl substances (PFAS), along with the pharmaceuticals carbamazepine and topiramate, were revealed to be good markers for tracing anthropogenic contamination in ground- and seawater, in concrete situations (e.g., highly contaminated sites). Additionally, non-target analysis expanded the number of potential tracers, making it a promising tool for identifying both the source and the fate of pollutants.

* Corresponding authors.
E-mail addresses: ruben.gil@idaea.csic.es (R. Gil-Solsona), pablo.gago@idaea.csic.es (P. Gago-Ferrero).

https://doi.org/10.1016/j.jhazmat.2023.130876
Received 23 September 2022; Received in revised form 11 January 2023; Accepted 25 January 2023
Available online 26 January 2023

1. Introduction

Human beings have always made use of the freshwater provided by aquifers. Unfortunately, anthropogenic activities have also negatively impacted groundwater (GW), which represents about 99% of the worldwide liquid freshwater (FW) [35]. Pollution is depleting the quality of this essential resource. In fact, more than 300 chemicals (pharmaceuticals, pesticides or disinfection by-products among others) have been detected in groundwater and/or drinking water to date [5]. The presence of chemicals of emerging concern (CECs) in these systems may have an impact on aquatic life and human health, even at low concentration levels [63]. Thus, both from an environmental and human health perspective, it is paramount to characterize the presence and fate of CECs in aquifers. Unfortunately, physicochemical and biological transformation of CECs in groundwater is poorly understood. This is especially true in coastal aquifers, where mixing of the usually oxic or suboxic fresh GW with the usually anoxic saline GW leads to high reactivity conditions [49,57], which may contribute to the transformation of CECs in coastal systems.

Two complementary processes occur along the coast: (1) Seawater intrusion (SWI) and (2) Submarine groundwater discharge (SGD). SWI refers to the landwards displacement of the subterranean freshwater/saltwater interface, which salinizes aquifer freshwater. GW exploitation lowers water levels and enhances SWI, thus threatening coastal aquifers worldwide [18]. SGD refers to the aquifer discharge of fresh GW, circulated seawater, or their mixture [44]. SGD is important for coastal biogeochemical cycles [52]. SGD is also becoming a source of global concern [68].

SWI is complex because of the density dependence of water flow and its sensitivity to heterogeneity, which, together with its relevance and ubiquity, has motivated numerous hydrologists to strive to understand it. SWI has been profusely studied from a theoretical and numerical point of view [33,38,48,8], as well as by means of laboratory tank simulations [29,65]. In-situ analyses of SWI are possible by means of hydraulic, chemical, electrical and thermal measurements. Therefore, SWI is a multidisciplinary topic which includes other disciplines such as geology, [1,66], geophysics [16,19,25], hydrodynamics [11,30,64] or hydrochemistry [45,59].

Because the impact of SGD on the dynamics and composition of the oceans was previously considered negligible, the study of SGD is a relatively new phenomenon. This misconception, along with the difficulties associated with implementation, delayed SGD assessments until the mid-1990 s [44,60]. It is now widely acknowledged that SGD plays an essential role in the dynamics of marine ecosystems, as it represents a relevant source of nutrients, trace metals and contaminants [52,61]. This source may be essential for many coastal habitats but may also negatively impact coastal ecosystems [4]. An excessive nutrient load may lead to eutrophication. SGD may also account for a wide variety of pollutants affecting the sea, many of them potentially persistent [52]. Therefore, it is not surprising that marine scientists have been paying more attention in recent times to SGD, investigating suitable tracers for identifying and quantifying chemical fluxes driven by SGD [44]. Radioactive isotopes of Ra or Rn, silica, or the salinity gradient, have been used for this purpose [17,23,53], but their applicability is limited. A more comprehensive picture can be gained by coupling traditional hydrological methods (e.g., hydraulic calculations, seepage meters) with alternative and complementary tracers [60]. We share the view of Adyasari et al. [2], that organic chemicals, including CECs, represent a threat but also an opportunity to gain understanding about SGD processes [2].

Several sources for the presence of CECs in the sea have been identified, including atmospheric deposition, surface water inputs or groundwater discharges [10,32]. But only a few studies have evaluated the role of SGD as a source of CECs in coastal seawater [41,42,58]. Furthermore, they focused on a limited number of chemicals, barely assessing their transformation under coastal aquifer conditions. The high reactivity of the seawater-freshwater interface suggests that many CECs will be transformed. In summary, the behavior of CECs in coastal and marine environments, their ultimate compartment, has been poorly studied in comparison to other water bodies such as sewage water or surface freshwater [10,24,6].

We find it self-evident that traditional target strategies need to be complemented with a broad range of organic compounds to properly understand the presence, distribution, transformation, and mobility of pollutants in costal systems. In this context, recent advances in high-resolution mass spectrometry (HRMS) facilitate a more holistic characterization of chemicals by expanding the available domain [21]. This non-target analytical strategy is applied after a sample pre-treatment focuses on quantitatively extracting as many chemicals as possible. Based on the exact mass and the information provided by the high resolution (HR) data, the substances of interest are statistically prioritized and can be tentatively identified. The retrospective character of this analytical tool should be highlighted. Hence, with this forward-looking approach, analysis is not limited to the data provided by the current research environment, as it will allow the evaluation of additional substances of interest at a future time and without the need to run further data acquisitions [43].

The purpose of this study is to take advantage of recent advances in HRMS analysis, combining wide-scope target (>2000 chemicals) and non-target strategies, to broaden the understanding of coastal aquifer systems regarding (1) SGD relevance as a source of organic CECs to the sea, by identifying chemicals present in coastal groundwaters and their reactivity in the mixing zone, and (2) the identification of chemicals which could potentially act as SGD tracers. To this end, groundwater (n = 17) and seawater (n = 2) samples were taken from a coastal site, located on the Spanish Mediterranean Coast, near Barcelona. The site has been extensively studied in an effort to characterize SWI and SGD at a typical Mediterranean coastal plain. As a result, it is characterized in terms of geology, hydraulics, biogeochemistry, geophysics, and hydrochemistry [13,14,20,28,27,40,46]. This site is therefore apt to test and evaluate the analytical methodologies we are proposing here.

2. Material and methods

2.1. Chemicals and materials

Methanol (MeOH) (HPLC-grade), water (HPLC-grade), formic acid (>99% purity) and hydrochloric acid (HCl) (37%) were purchased from Merck (Darmstadt, Germany). Distilled water was obtained by a Milli-Q purification system (Aurium, PRO-VFT, Sartorius, Göttingen, Germany). Ammonium acetate was acquired from Merck. Analytical standards, including the internal standards (IS), were purchased from Sigma-Aldrich (Steinheim, Germany) and LGC Standards (Barcelona, Spain). Further information regarding analytical standards and ISs was summarized in the supplementary data (Table A.1, **SI-1**). A mix of ISs (1 ppm) was prepared by mixing appropriate aliquots of each standard stock solution in MeOH. Water samples were filtered through Whatman™ Glass Microfiber Filters (GF/F) 0.7 μm, 47 mm. SPE cartridges Bond Elut-PPL (500 mg, 6 mL) from Agilent were also used.

2.2. Site description and sampling

2.2.1. Site description and characterization

The experimental site is located along the Maresme coastal plain, specifically in the alluvial aquifer of the Argentona ephemeral stream (Barcelona, Spain; 41°31′11.2″ N, 2°25′25.3″ E) (Fig. 1a). The climate is typically Mediterranean, marked by warm, dry summers and wet, mild winters. Precipitation ranges from around 600 mm/y at the plain to some 700 mm/y in the coastal range behind the plain. Rainfall is unequally distributed. It concentrates in spring and, especially, autumn, when monsoon-like rainfall events cause floods, the only occasion when the stream actually flows to the sea. The stream runs between

agricultural fields on the SW side and the city of Mataró (actually its suburban industrial zone) to the NE. The wastewater treatment plant (WWTP) of the city is located adjacent to the stream, some 300 m upstream from the site. Its effluent discharges some 2000 offshore through an outfall that runs close to the site. Some effluent may leak off the outfall into the aquifer. Moreover, the sewer system of Mataró is unitary (it collects both wastewater and surface runoff) and bypasses the WWTP when the flow rate exceeds the WWTP capacity during storms, causing some untreated wastewater, diluted by surface runoff, to infiltrate the aquifer.

Characterization of the sited involved drilling 17 piezometers on the right bank of the stream. These piezometers allowed for monitoring heads and collecting groundwater samples along the freshwater-seawater mixing zone (often referred to as subterranean estuary for the marine science community). The piezometers used in this study were located along a section perpendicular to the Mediterranean Sea, at distances ranging from 18 to 102 m to the shoreline and depths from 7 to 22 m below the ground surface. Except for two stand-alone piezometers (PP10 and PP18), piezometers were grouped in nests (N1, N2, N3 and NMar) consisting of 3–4 piezometers of different depths (Fig. 1b) to facilitate monitoring and testing along the vertical course, so as to best characterize vertical mixing processes. Most piezometers were equipped with pressure sensors, as well as distributed temperature sensors and electrodes attached to the outside of the PVC tubing (see [20] for details). The tubing (casing) was slotted over a short 2 m interval, adjacent to sandy sediments, to minimize mixing within the piezometer and during sampling, leaving at least 2 m of blind pipe at the bottom of the casing.

The main findings relating to the hydrogeological context are summarized in Fig. 1. The aquifer consists of sandy fluvial layers separated by thin silty layers. Fluvial deposits overlie weathered granite of low permeability but are often underlaid by a conductive layer at the point of contact between the weathered and unweathered granite [39], below the monitored section. Freshwater (FW) discharges sub-horizontally into the sea, along the sand layers and vertically across the silt layers. Seawater (SW) flows within the aquifer under the influence of three mechanisms: (1) according to the traditional SWI paradigm, the dense SW flows onshore at depth due to its relatively high density, and returns seawards with a sharp turn as it mixes with FW; (2) SW enters near the shore due to storm surges, and; (3) SW fingers down into FW zones, and vice versa, due to tidal fluctuations and the instability caused by the dense SW overlying the light FW.

The location and extent of the FW flow paths below the silt layers, which hold SW above, has been ascertained by Electrical Resistivity Tomography [46], induction logging [40], and tidal response analyses [27]. This is shown in Fig. 1, where water is divided according to the traditional definition in fresh (salinity less than 1 PSU, Practical Salinity Units), brackish (salinity between 1 and 10 PSU) and saline (salinity greater than 10 PSU). Note however that the salinities we have measured within the aquifer are well below Mediterranean Sea salinities (averaging 38 PSU at our site). Also, the diffuse and unstable nature of FW SGD makes it very difficult to sample actual SGD. Instead, what we sample is GW next to the sea, close to its discharge point, as well as two superficial seawater samples in the zone influenced by SGD.

2.2.2. Sampling

Sampling was carried out during three consecutive days in December 2021. Autumn is usually the wettest period of the year, so that groundwater levels are usually highest during December. Even if 2021 was a relatively dry year, heavy storms which occurred in October contributed to the explanation of the distribution of salinities in the aquifer. Sampling was performed according to standard protocols. In short, firstly a submersible pump was placed at the screened intervals of the piezometers to extract groundwater, and a multi-parameter probe with a flow cell was connected to the pump to measure in-situ temperature, dissolved oxygen (DO), pH, redox potential (ORP) and salinity. Second, three times the volume of the screened interval of the piezometer for each sampling point was purged. Third, pumping continued at a constant rate, until some 4.5 L had been collected, filtered through 20 μm in-situ and stored at 4 °C in amber glass bottles (pre-cleaned with acetone and Milli-Q water, and rinsed with the sampling point groundwater twice). Additionally, two surface seawater samples were taken offshore at 60 and 130 m from the shoreline in the direction aligned with the piezometers. Field blanks (n = 3) analyses were performed with 4 L of Milli-Q water every sampling day. Additional data regarding the sampling sites, including shoreline distance, depth, and in-situ measured parameters, is provided in Table A.2 (SI-2).

2.3. Sample preparation and instrumental analysis

The water samples (4L) were filtered through glass fiber filters (pore size 0.7 μm, Whatman GF/F, pre-heated (450 °C, 4 h)) and the pH was adjusted to 2 with HCl. Then, two isotopically labeled chemicals (benzotriazole-d4 and methyl-paraben-d3) were added as surrogate to ensure good SPE reproducibility. PPL columns were activated by leaving them to soak in 3 mL of methanol overnight. Methanol was then drained and 3 mL of Milli-Q water (pH=2, HCl) was passed through for column conditioning. Filtered samples were loaded onto the PPL columns and eluted (< 3 mL·min^{-1}). Salts were subsequently removed from the PPL columns by passing 6 mL of Milli-Q water (pH=2, HCl). Next, the cartridges were dried under vacuum for 20 min and further eluted with 3 mL of methanol. The extract volume was finally adjusted to 2 mL with

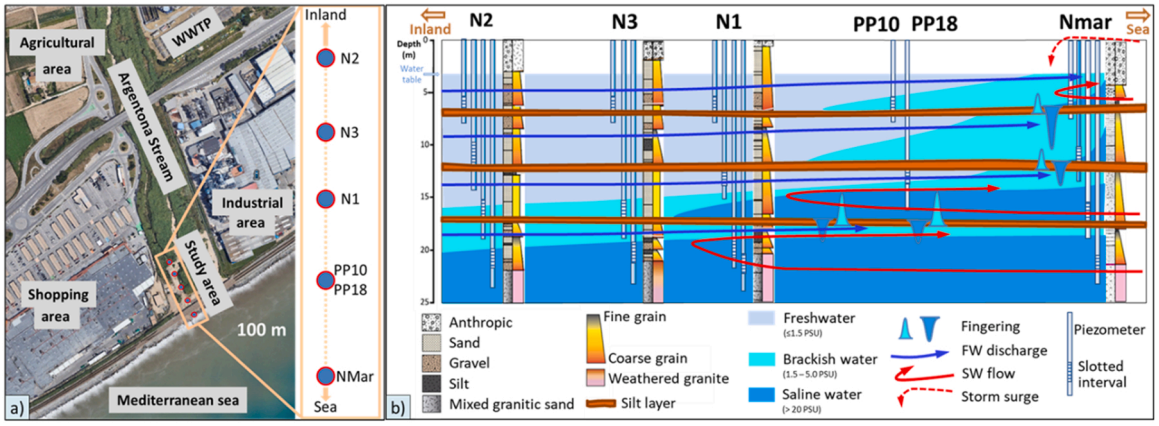

Fig. 1. Site description. A) Google Earth image of the site, including location of sampling piezometers (red circles near the shore) and land use. B) Schematic vertical cross-section, including slotted intervals, lithology, grain size, flow patterns, and water salinity (fresh, brackish, and saline) zones.
Adapted from [40].

HPLC-grade MeOH and stored at − 20 °C pending analysis. Before analysis, samples were diluted (1:1, v/v) with HPLC-grade water and the IS mix was added (Table A.1, SI-1) to correct for matrix effects.

Instrumental analysis was performed using an Acquity UHPLC system (Waters, Milford, USA) coupled with a Q-Exactive Orbitrap mass analyser (Thermo Fisher Scientific, Dreieich, Germany). The chromatographic separation was carried out by a Waters Cortecs C18 (2.1 ×100 mm, 2.7 μm) column headed by a Waters Cortecs C18 (2.1 ×5 mm, 2.7 μm) precolumn. An electrospray ionization (ESI) interface operated at 3000 and 2800 V in positive and negative mode, respectively. Instrumental parameters for ESI were: 350 °C capillary temperature, 40 sheath gas flow, 10 auxiliary gas flow, 100 of maximum spray current, 350 °C probe heater temperature and 60 SLens RF level. In positive ionization mode, HPLC-grade water (aqueous phase) and methanol (organic phase), both with 0.1% formic acid, were employed as a mobile phase, and underwent the following elution gradient: 5–75% B (0–7 min), 75%− 100% B (7–10 min), 100% B (10–17 min), 100–5% B (17–18 min). In negative ionization mode, HPLC-grade water (aqueous phase) and methanol (organic phase), both with 5 mM ammonium acetate, followed the elution gradient described here: 5–50% B (0–3 min), 50%− 90% B (3–6 min), 90–100% B (6–13 min), 100% B (13–17 min) and 100–5% B (17–18 min). In both modes, a constant flow of 0.3 mL·min^{-1}, an injection volume of 5 μL and, a constant column temperature of 40 °C was applied. The instrument executed two acquisition modes: data independent (DIA) and data dependent acquisition (DDA). DIA consisted of a full scan with low collision energy (4 eV) and a full scan with a high collision energy (25 eV), in a mass-to-change ratio (*m/z*) range from 67 to 1000 and resolving power of 60,000. In contrast, DDA mode acquired full scans at low collision energy (4 eV), and MS^2 spectra for the 5 most intense ions in each scan were, then, registered (35 eV applied as collision energy and 30,000 as resolving power), excluding those ions previously selected in the last 30 s

2.4. Target and non-target analysis and data processing

Data Independent Acquisition (DIA) files were converted to ".mzml" files with MSConvert (Table A.3, SI-3). Target and non-target strategies were applied to assess the presence of organic pollutants and possible organic tracers in the aquifer, as described below. The target and non-target performance workflow is illustrated in Fig. A.1, SI-3.

2.4.1. Target analysis

Target analysis evaluation was conducted for 748 chemicals (Table A.1, SI-1) in a similar manner as described elsewhere [22]. Raw files were processed with MZMine2 software [47]. Parameters and workflow for MZMine2 are summarized in Table A.4, SI-3.

Only the chemicals meeting the following criteria were reported as positive findings: i) Peak area in the samples > summatory of the field blank peak area for each sampling day plus three times the standard deviation; ii) Peak area for the parent ion (and its main fragment ion, when available) > 5E5 in the most intense sample (to avoid the occurrence of false positives due to interferences or noise).

2.4.2. Non-target-based prioritization strategy and identification of unknowns

In the non-target workflow, generic (.mzml) files were imported to MZMine2 and a mass list for each scan was generated. Parameters and workflow for MZMine2 are summarized in Table A.5, SI-3. The final table was exported to a ".csv" file and blank subtraction was performed in the same manner described in the target approach. Finally, a correlation between the salinity levels and each feature at all the sampling points was calculated. The features with a R^2 higher than 0.7 were prioritized. The feature list was exported to SIRIUS4.20 [15]. Both molecular formula and tentative compound annotations were obtained, based on the information on accurate mass, isotopic pattern, and the high-energy MS^2 spectra. In all cases the tentative identifications were manually checked, and, when available, compared with the spectra observed in databases including MassBank, MassBank of North America, Metlin, HMDB and mzCloud. MetFrag was also used for in silico fragment annotation in some identifications [50,51]. The identification confidence was reported using the hierarchical levels previously described by Schymanski et al., [54]. In all cases, procedural blanks were carefully assessed to avoid false positives.

3. Results and discussion

3.1. Occurrence and distribution of the target chemicals in the aquifer

A total of 92 chemicals out of the 748 initially targeted were detected in the aquifer (Table 1) and their abundance is represented as a clustered heatmap in Fig. A.2, SI-4. A wide variety of industrial chemicals were determined in the groundwater under study, including plastic additives (e.g., bisphenol AF, phthalates), perfluoroalkyl substances (e.g., PFOA, PFOS), surfactants (e.g., oleamide, lauryl sulfate), flame retardants (e.g., Tris(1-chloro-2-propyl) phosphate), and benzothiazoles and benzotriazole derivatives, among others. Also, several pharmaceuticals (e.g., carbamazepine, dextrorphan), personal care products (e.g., cetrimonium, ensulizole), food-related compounds (e.g., caffeine), biocides (e.g., atrazine, clothianidin) and drugs of abuse (e.g., cocaine and its metabolite benzoylecgonine) were detected. These compounds suggest a broad range of sources, ranging from infiltrated surface runoff or waste water, return flow of irrigated lands, or legacy industrial pollution [62]. Among these anthropogenic chemicals, a general decrease in abundance of those compounds, was observed with the increase of salinity, due to the higher proportion of seawater.

In seawater samples, a total of 44 chemicals were detected. Although in most cases they showed the lowest abundances among all the evaluated sampling sites (Fig. A.2, SI-4), it indicated that a high number of chemicals were present in the coastal waters, which was in line with the data reported by the few other studies carried out in the field [3,7]. However, the observed minor variations may be due to the difference in the biogeochemical processes taking place in the mixing zone.

Regarding SGD processeses, target substances with the potential to provide useful information were priorized (Fig. 2). Out of the detected target compounds, a total of 32 chemicals were present in more than 75% of the analyzed aquifer samples. Only these 32 chemicals were prioritized as potential tracers, as their presence in a high number of samples indicates persistence under aquifer conditions. Thus, their peak area in the chromatograms, directly related with their abundance, were compared with the salinity values (Table A.2, SI-2) to find those that linearly correlate. In this manner, two linear regressions (salinity vs corrected peak area and Ln(salinity) vs corrected peak area) were performed. The term "corrected peak area" refers to the peak area of each compound corrected by the peak area of the IS. Eight anthropogenic chemicals followed a reverse trend with salinity (R^2 >0.7) (Table 2). These chemicals were of special interest as their abundance decreased mainly as a consequence of dilution, indicating a minimum degradation. These compounds included 6 perfluoroalkyl substances (PFAS, also known as 'forever chemicals'), that followed similar and consistent trends among them, and two pharmaceuticals: topiramate and carbamazepine (CBZ). All of them are highly recalcitrant chemicals and therefore little affected by physicochemical degradation processes within the aquifer. Consequently, its distribution in the different zones of the aquifer might help in monitoring the aquifer system and freshwater SGD, if they indeed behave as conservative tracers for monitoring SGD.

The spatial distribution of the whole amount of PFAS throughout the aquifer, as well as the specific distribution of PFOS, are represented in Fig. 3**a** and Fig. 3**b**, respectively. PFAS commonly enter the environment through production or contaminated waste streams. PFAS are highly mobile and can be easily transported through the aquifer. Their presence

Table 1
Chemicals detected in the aquifer.

Compound	Molecular formula	Type of product/industrial category	RT (min)	DR%[b]	IM[c]	LogP[d]
			ESI (+) / ESI (-)			
1,3-Dicyclohexylurea	C13H24N2O	Tire rubber – derived contaminants	7.49 / n.a.	94	+	3
1,3-Diphenylguanidine	C13H13N3	Accelerator in rubber industry	2.97 / n.a.	100	+	2.4
1 h,1 h,2 h,2 h-perfluorooctanesulfonic acid	C8H5F13O3S	PFAS	n.a. / 5.41	12	-	3.9
1 H-Benzotriazole	C6H5N3	Anticorrosion agent	3.76 / 3.22	100	+ / -	1
2,4,6-trimethylbenzenesulfonic acid	C9H12O3S	Industrial chemical	n.a.[a] / 3.34	82	-	1.8
2-Benzothiazolesulfonic acid	C7H5NO3S2	Benzothiazole family	n.a. / 2.57	94	-	1.5
2-Hydroxybenzothiazole	C7H5NOS	Benzothiazole family	5.46 / 4.34	100	+ / -	1.8
3,5-di-tert-butyl-4-hydroxybenzaldehyde	C15H22O2	Benzaldehyde family	8.64 / n.a.	41	+	4.4
4-Acetamidoantipyrine	C13H15N3O2	Pharmaceutical (metabolite)	3.34 / n.a.	88	+	0
4-Dodecylbenzenesulfonic acid	C18H30O3S	Surfactant	n.a. / 6.73	47	-	7
4-formylaminoantipyrine	C12H13N3O2	Pharmaceutical (metabolite)	3.27 / n.a.	41	+	0
4-Hydroxybenzoic acid	C7H6O3	Preservative	n.a. / 1.85	18	-	1.6
4-Methyl-1 H-benzotriazole	C7H7N3	Benzotriazol family	4.98 / 4.02	100	+ / -	1.4
4-Nitrophenol	C6H5NO3	Manufacture drugs / biocides	n.a. / 3.64	29	-	1.9
4-Octylphenol	C14H22O	Surfactant	n.a. / 6.94	41	-	5.3
5-Chlorobenzotriazole	C6H4ClN3	Benzotriazol family	n.a. / 4.25	100	-	1.7
6-(methoxyphenyl)pyrimidine-2,4-diamine	C11H12N4O	Member of pyrimidines	2.23 / n.a.	12	+	1.1
Acridine	C13H9N	Dyes/coating	4.06 / n.a.	29	+	3.4
Acridone	C13H9NO	Acridine derivarive	6.07 / n.a.	12	+	3
Antipyrine	C11H12N2O	Pharmaceutical	4.30 / n.a.	100	+	0.4
Atrazine	C8H14ClN5	Biocide	6.81 / n.a.	35	+	2.6
Atrazine-desisopropyl	C5H8ClN5	Biocide	3.80 / n.a.	82	+	1.1
Benzoic acid	C7H6O2	Preservative	n.a. / 1.56	53	-	1.9
Benzothiazole	C7H5NS	Rubber production	6.04 / n.a.	29	+	2
Benzoylecgonine	C16H19NO4	Drugs of abuse (metabolite)	3.71 / n.a.	71	+	-0.3
Bisphenol AF	C15H10F6O2	Plastic additive	n.a. / 5.80	24	-	4.5
Bisphenol S	C12H10O4S	Plastic additive	4.73 / 3.65	18	+ / -	1.9
Caffeine	C8H10N4O2	Food related chemical	3.59 / n.a.	12	+	-0.1
Caprolactam	C6H11NO	Synthesis of fibers	3.23 / n.a.	12	+	-0.1
Carbamazepine	C15H12N2O	Pharmaceutical	6.33 / n.a.	88	+	2.5
Cetrimonium	C19H42N+	Surfactant, PCPs	8.54 / n.a.	12	+	8
Clothianidin	C6N5H8SO2Cl	Biocide	n.a. / 3.37	53	-	1.3
Cocaine	C17H21NO4	Drugs of abuse	3.47 / n.a.	71	+	2.3
Cotinine N-oxide	C10H12N2O2	Tobacco related chemical	0.96 / n.a.	35	+	-1.3
Decaethyleneglycol	C20H42O11	Petroleum derivate	4.32 / n.a.	12	+	n.a.[e]
Desethylterbuthylazine	C7H12ClN5	Biocide (metabolite)	6.27 / n.a.	82	+	2
Desvenlafaxine	C16H25NO2	Pharmaceutical	3.38 / n.a.	94	+	2.6
Dextrorphan	C17H23NO	Pharmaceutical	3.37 / n.a.	29	+	3.1
Dibutyl phosphate	C8H19PO4	Antifoaming agent, catalyst	8.85 / n.a.	82	+	1.5
Diethyltoluamide	C12H17NO	Biocide	6.95 / n.a.	53	+	2
Diisobutyl phthalate	C16H22O4	Plastic additive	8.97 / n.a.	24	+	4.1
Dimethyl phthalate	C10H10O4	Plastic additive	5.75 / n.a.	35	+	1.6
Dimethyl sebacate	C12H22O4	Plastic additive	6.33 / n.a.	24	+	3
Di-n-Butyl phtalate	C16H22O4	Plastic additive	9.07 / n.a.	24	+	4.7
Diuron	C9H10Cl2N2O	Biocide	6.92 / 5.30	82	+ / -	2.7
Dodecaethylene glycol	C24H50O13	Petroleum derivate	4.72 / n.a.	12	+	n.a.
Ensulizole	C13H10N2O3S	PCPs (sunscreen agent)	3.30 / n.a.	59	+	2
Icaridin	C12H23NO3	Insect repellant	7.17 / n.a.	41	+	2
Imidacloprid	C9H10ClN5O2	Biocide	4.09 / n.a.	53	+	1.2
Lamotrigine	C9H7Cl2N5	Pharmaceutical	3.29 / n.a.	71	+	1.4
Laurolactam	C12H23NO	Synthesis of fibers	7.40 / n.a.	24	+	2.8
Lauryl diethanolamide	C16H33NO3	Personal care product	8.77 / n.a.	35	+	3.5
Lauryl sulfate	C12H26O4S	Surfactant	n.a. / 6.28	12	-	4.7
Lidocaine	C14H22N2O	Pharmaceutical	2.40 / n.a.	41	+	2.3
Metalaxyl	C15H21NO4	Biocide	6.87 / n.a.	59	+	1.6
Metolachlor ethanesulfonic acid	C15H23NO5S	Biocide	7.70 / n.a.	53	+	1.4
N-Butyldiethanolamine	C8H19NO2	Neutralizing additive	0.81 / n.a.	29	+	0.1
Nicotine	C10H14N2	Tobacco related chemicals	0.78 / n.a.	71	+	1.2
Octapropylene glycol (PPG n8)	C24H50O9	Moisturizer	7.79 / n.a.	18	+	1
Octyl hydrogen phthalate	C16H22O4	Plastic additive	8.91 / n.a.	24	+	5.3
Oleamide	C18H35NO	Surfactant	10.42 / n.a.	59	+	6.6
Oxindole	C8H7NO	Natural product	4.22 / n.a.	29	+	1.2
Pentaethylene Glycol	C10H22O6	Petroleum derivate	2.67 / n.a.	18	+	n.a.
Pentapropylene glycol (PPG n5)	C15H32O6	Moisturizer	6.05 / n.a.	59	+	0.2
Perfluoro-1-butanesulfonamide	C4H2F9NO2S	PFAS	n.a. / 4.92	71	-	2.2
Perfluorobutanesulfonic acid (PFBS)	C4HF9O3S	PFAS	n.a. / 4.16	88	-	2.3
Perfluorodecanoic acid (PFDA)	C10HF19O2	PFAS	n.a. / 6.15	53	-	6.3
Perfluoroheptanesulfonic acid (PFHpS)	C7HF15O3S	PFAS	n.a. / 5.56	71	-	4.3
Perfluoroheptanoic acid (PFHpA)	C7HF13O2	PFAS	n.a. / 5.17	88	-	4.3
Perfluorohexanesulfonate (PFHxS)	C6F13O3S-	PFAS	n.a. / 5.19	100	-	3.6
Perfluorohexanoic acid (PFHxA)	C6HF11O2	PFAS	n.a. / 4.68	100	-	3.6
Perfluorononanoic acid (PFNA)	C9HF17O2	PFAS	n.a. / 5.88	65	-	5.6
Perfluorooctanesulfonic acid (PFOS)	C8HF17O3S	PFAS	n.a. / 5.87	76	-	5

(*continued on next page*)

Table 1 (*continued*)

Compound	Molecular formula	Type of product/industrial category	RT (min) ESI (+) / ESI (-)	DR%[b]	IM[c]	LogP[d]
Perfluorooctanoic acid (PFOA)	C8HF15O2	PFAS	n.a. / 5.56	88	-	4.9
Perfluoropentanesulfonic acid (PFPeS)	C5HF11O3S	PFAS	n.a. / 4.74	71	-	3
Perfluorovaleric acid (PFPeA)	C5HF9O2	PFAS	n.a. / 4.00	88	-	2.9
Phendimetrazine	C12H17NO	Pharmaceutical	7.24 / n.a.	53	+	1.9
Pilocarpine	C11H16N2O2	Pharmaceutical	0.94 / n.a.	82	+	1.1
Ritalinic acid	C13H17NO2	Pharmaceutical (metabolite)	3.37 / n.a.	88	+	-2.4
Simazine	C7H12ClN5	Biocide	6.16 / n.a.	82	+	2.2
Stearic acid	C18H36O2	Surfactant	n.a. / 8.28	35	-	7.4
Tapentadol	C14H23NO	Pharmaceutical	8.32 / n.a.	76	+	3.5
Tetradecylsulfate	C14H29O4S-	Surfactant	n.a. / 6.81	6	-	5.8
Tetrapropylene glycol (PPG n4)	C12H26O5	Moisturizer	5.10 / n.a.	47	+	-0.1
Topiramate	C12H21NO8S	Pharmaceutical	n.a. / 4.15	76	-	-0.8
Tributyl phosphate	C12H27O4P	Flame retardant	8.98 / n.a.	71	+	2.9
Triethyl citrate	C12H20O7	Coatings, additive, PCPs	6.02 / n.a.	18	+	0.1
Triethyl phosphate	C6H15O4P	Industrial use	5.38 / n.a.	82	+	0.8
Triphenylphosphine oxide	C18H15OP	Rubber additive	7.37 / n.a.	100	+	2.8
Tris(1-chloro-2-propyl) phosphate	C9H18Cl3O4P	Flame retardant	7.54 / n.a.	35	+	3.3
Valproic acid	C8H16O2	Pharmaceutical	n.a. / 4.29	100	-	2.8
Xylenesulfonate	C8H9O3S-	Surfactant	n.a. / 2.79	76	-	1.3

[a] n.a.: non-ionizable in this mode. [b]Detection rate (DR%) accounting for the chemicals detected in the groundwater samples (detected chemicals in the groundwater samples divided by the total groundwater samples). [c]Ionization mode (IM) in ESI (positive=+ and/or negative=-). [d]Logarithm of the octanol-water partition coefficient (LogP) computed by XLogP3 3.0 (PubChem release 2021.05.07). [e]N/A = non-available.

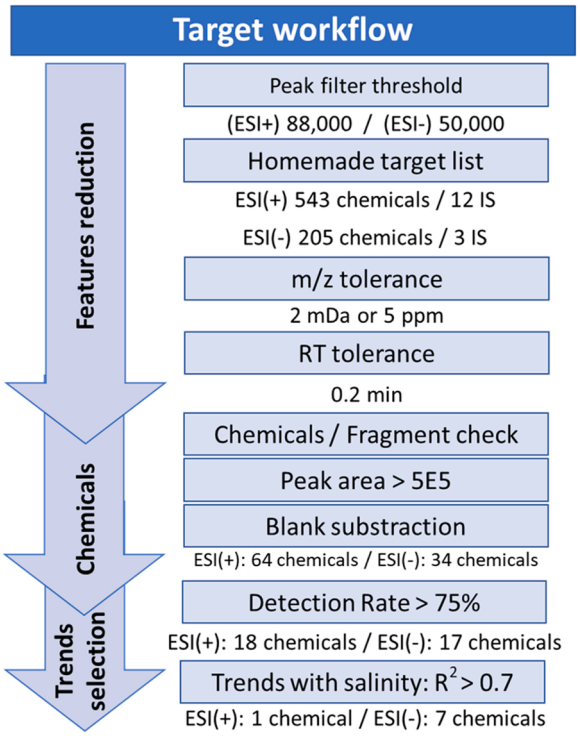

Fig. 2. Screening and prioritization target workflow.

has been previously reported in groundwater from different regions in concentrations ranging from low pg·L^{-1} to low mg·L^{-1} [56]. In this study, PFOA and PFOS were the most abundant within the PFAS family of chemicals, which is consistent with other studies in surface and groundwater [34,56]. Due to their persistent behavior and high ionization efficiency in negative electrospray ionization mode (which leads to low limits of detection), these substances may be useful tracers for the mobility of organic chemicals within the aquifer. PFAS were present at higher levels in the shallowest sites, especially in N2–10 and N1–10, which were highly influenced by surface water infiltration, but also at deep samples, which suggests origination and transport from further afield. According to these results and their intrinsic properties, PFAS

Table 2
Chemicals which followed a trend (Coefficient of Determination (R^2) > 0.7) with salinity values. R^2 for a linear regression between salinity and corrected peak area (C) and a linear regression between $ln_{salinity}$ and C, is included.

Family	Chemicals	R^2 (Salinity VS C)	R^2 ($ln_{Salinity}$ VS C)
PFAS	PFHpA	0.875	0.857
	PFBS	0.872	0.794
	PFHxA	0.821	0.777
	PFOS	0.876	0.882
	PFOA	0.831	0.825
	PFPeA	0.810	0.818
Pharmaceuticals	Topiramate	0.717	0.721
	Carbamazepine	0.741	0.590

could also be potentially useful for tracing SGD. However, these chemicals are consistently found at low concentrations in seawater [56,67], even in remote environments such as the Antarctic region or the Arctic Ocean [9,36]. Therefore, the low levels determined in the coastal sea, close to the detection limits, prevented the presence of PFAS from being attributed to groundwater input. This also led to the suggestion that PFAS might not be a good SGD tracer in the hydrogeological and coastal context. Its potential application should be limited to highly PFAS-contaminated groundwater systems, where the concentration of these chemicals could be easily traced in the seawater above the basal levels, which are usually found at pg·L^{-1} level [26,36]. Another context in which they might feasibly function as trackers is in marine zones with a high proportion of freshwater, such as karstic or volcanic systems or semi-closed coastal areas (e.g., coastal lagoons or coves).

The pharmaceuticals carbamazepine (Fig. 3c) and topiramate (Fig. A.3, SI-4), both employed as anticonvulsants, followed the same reversal trend in concentration with salinity as PFAS. These chemicals were also present in the fresh-water samples. Their abundance was much lower in the deep aquifer samples rich in SW and absent (below the limit of detection) in the seawater sites. These results were in line with previous studies that proposed carbamazepine as an anthropogenic marker during groundwater infiltration from wastewater treatment processes because of its persistence, as it was assumed that it is not subjected to degradation or adsorption under these conditions [12,31].

Regarding topiramate, the available information in the literature is much scarcer, but it is expected to persist in aquatic environments. Therefore, it could be proposed as another potential infiltration tracer in

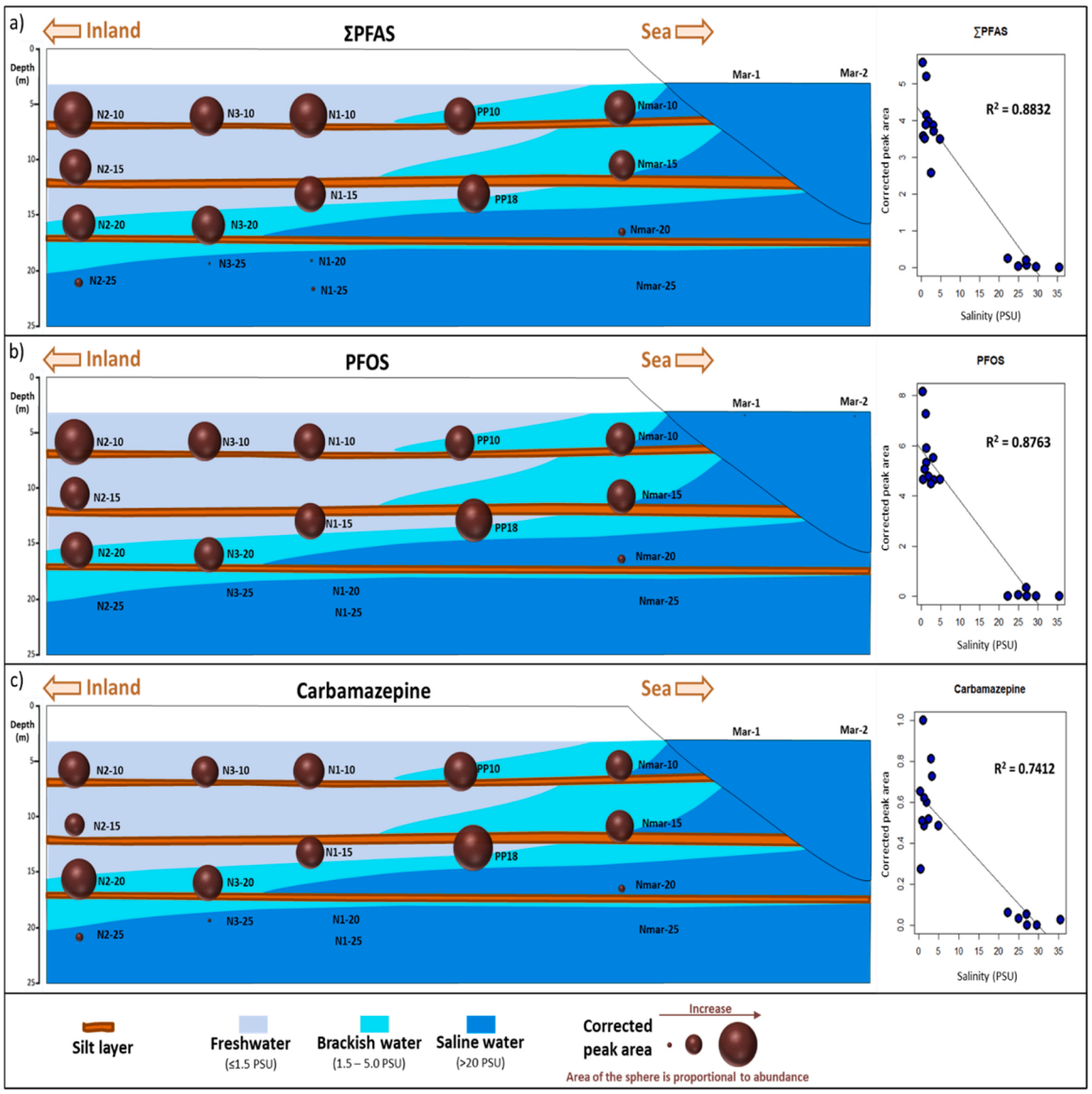

Fig. 3. Distribution of PFAS, PFOS and carbamazepine along the aquifer. Fresh, brackish, and saline water were represented among with the silt layers which (semi) confined the system [40]. a) Distribution of the overall amount (normalized) of PFAS, including PFHpA, PFBS, PFHxA, PFOS, PFOA, PFPeA and its linear regression versus salinity. b) Distribution of PFOS and its linear regression versus salinity. c) Distribution of carbamazepine and its linear regression versus salinity.

aquatic environments, including SGD in systems highly affected by anthropogenic contamination, and thus, complement the use of carbamazepine. Other pharmaceuticals were also detected in the aquifer at different levels. Nonetheless, none of them, including those detected with a high DR% and intensity (e.g., valproic acid, desvenlafaxine), followed the same inverse trend relative to salinity as carbamazepine and topiramate, probably due to their higher biodegradability during the different transformation processes taking place under the aquifer conditions.

The abundance of the rest of the highly detected chemicals (DR% >75%) did not follow a reverse trend relative to salinity. Nevertheless, as mentioned above, their distribution throughout the different zones of the aquifer may be used to understand some of the processes taking place. In this regard, different zones within the aquifer were identified in terms of their salinity levels (Table A.2, SI-2). The freshwater zone (salinity less than 1.5 PSU) was characterized by low seawater influence and included the sampling sites N2–10, N2–15, N3–10, N1–10, N1–15 and PP18. The brackish zone (salinity ranged from 1.5 to 5.0 PSU) represents a zone where water contains a significant, but minoritarian, fraction of seawater included sampling sites N2–20, N3–20, PP10, NMar-10 and NMar-15. Finally, a saline zone (salinity greater than 20.0 PSU) with a high fraction of seawater, included the sites N1–20, NMar-20, N1–25, N2–25, N3–25 and NMar-25. A representative example of a distribution of chemicals not related to salinity can be found in benzotriazoles, which are widely used in the chemical industry as corrosion inhibitors, and were detected in all the aquifer samples (Fig. 4). Methylbenzotriazole and 5-chlorobenzotriazole were present at high levels in the freshwater end of the mixing zone (with a similar abundance in both) but with much smaller intensities in the shallow freshwater zone. This behavior could be explained by the different degradation rates expected for the different aquifer conditions in those areas, especially the redox state which could vary from oxidizing/aerobic to reducing/anaerobic. In addition, different transformation pathways have already been proposed for benzotriazoles and its methylated or chlorinated derivatives, which could also contribute to this scenario [37,55]. Results suggested that these chemicals were degraded under oxidizing conditions, which are predominant in the shallow freshwater zone. In the mixing zone, where silty layers semi-confined the aquifer and the

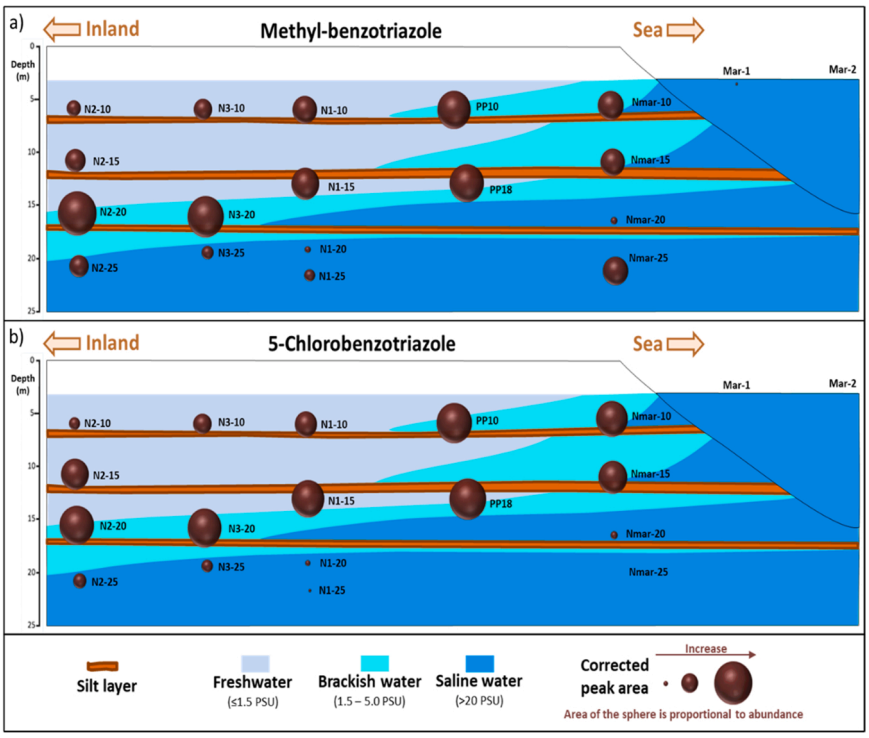

Fig. 4. Distribution of chemicals along the aquifer, including: a) methyl-benzotriazole and b) 5-chlorobenzotriazole.

environment is not that oxidizing (or is even reducing), the degradation was lower. In addition, the large seawater intrusion produced in the salty zone diluted the freshwater and, therefore, decreased the abundance of these two chemicals. However, previous studies suggested the existence of additional sources for these chemicals in the aquifer, such as runoff infiltration or input from wastewater treatment plants (WWTPs) [28], which would complicate the system dynamics.

3.2. Non-target prioritization and identification of unknowns

A total of 5543 features were detected in the aquifer after blank subtraction, and 1721 of them were present in more than 75% of the groundwater samples. In a similar manner as carried out in the target analysis, their peak area in the chromatograms was compared with the salinity values, to identify those with a linear correlation (R^2 >0.70). After eliminating matches already found in the target analysis, a total of 3 features (expressed as *m/z*, along with their detection rate (DR%), retention time (RT), ionization mode (IM) and R^2) were prioritized for further identification (Table 3).

The non-target workflow followed in the identifications (Fig. 5) provided 3 features. One chemical was tentatively identified as probable structure (Level 3) while another identification remained as exact *m/z* of interest (Level 5). One of the prioritized features was identified as in-source fragment associated to one of the aforementioned substances.

The first feature of interest was *m/z* 168.9883. This *m/z* value corresponded to one of the main common fragments resulting from PFAS and it co-eluted with several target chemicals of this family (e.g., PFOS, PFOA or PFNA). Additionally, this fragment coeluted with the prioritized feature *m/z*: 524.9597, which also presented a mass defect and an isotopic pattern characteristic of the PFAS family (Table 3). The feature presented a low intensity and coeluted with PFOS and PFNA, thus, a DDA injection with 50 μL injection volume was performed (Fig. 6). The fragments 418.9744, 218.9865,

Table 3
Non-target features detected in the aquifer samples whose peak area in the chromatograms followed a reverse trend with salinity values.

m/z (mDa)	RT[a] (min)	DR%[b]	R^2[c]		IM[d]	Molecular Formula	Tentative structure	Level[e]
			C vs Salinity	C vs $ln_{Salinity}$				
524.9597	5.87	82	**0.74**	**0.89**	-	$C_{11}HF_{19}O_2$	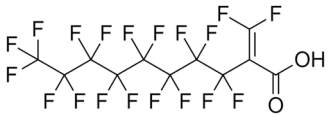	3
168.9883	5.7	82	0.58	**0.73**	-	$[C_3F_7]^-$	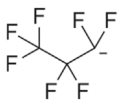	-
439.2931	7.12	100	**0.70**	0.54	-	n.a.[f]	n.a.	5

[a] Retention time (RT).
[b] Detection rate (DR) expressed as a percentage, accounting for the groundwater samples.
[c] Coefficient of determination (R^2) for the linear regression between salinity and corrected peak area (C) as well as a linear regression between $ln_{Salinity}$ and C.
[d] Ionization mode (IM), + or -, in ESI.
[e] Level of identification according with Schymanski et al. Schymanski et al., (2014) [54].
[f] n.a.: information non-available.

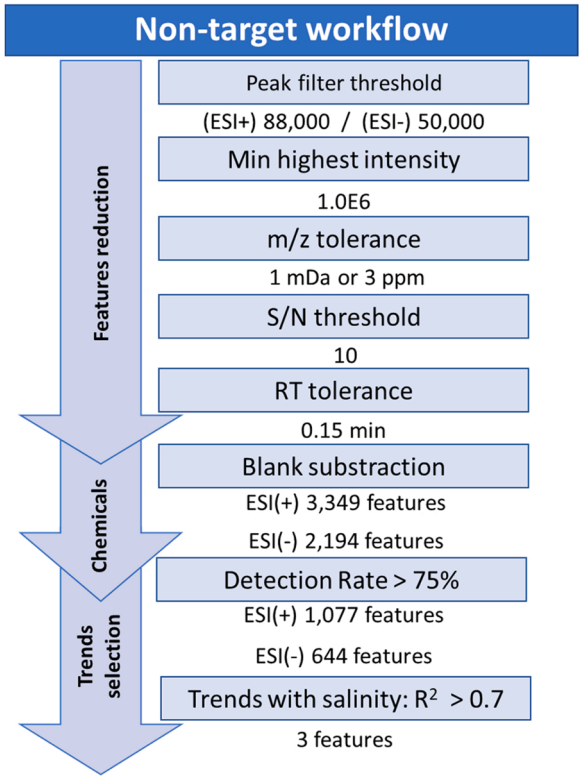

Fig. 5. Prioritization non-target workflow.

168.9897 and 118.9920 were finally assigned. Only one molecular formula (C11HF19O2) presented a plausible structure according to MetFrag and Sirius. Using PubChem database and a mass error threshold of 5 ppm, three structural isomers were proposed as possible: 2-(difluoromethylene)−3,3,4,4,5,5,6,6,7,7,8,8,9,9,10,10,10-heptadecafluoro-decanoic acid, (Z)−3,4,4,5,5,6,6,7,7,8,8,9,9,9-tetradecafluoro-2-(1,1,2,2,2-penta-fluoroethyl) non-2-enoic acid and 2-(difluoromethylene)− 3,3,4,4,5,5,6,6,7,7,8,9,9,9-tetradecafluoro-8-(trifluoromethyl)nonanoic acid. The first structure can explain all the proposed fragments, while the second and the third one could not explain the fragments *m/z* 418.9744 and 118.9920, respectively. Therefore, this chemical was considered tentatively identified (confidence level 3).

The identification of this chemical is consistent with the results obtained in the target analysis and reinforce the potential use of PFAS as tracers for fresh SGD in groundwater-polluted environments. Also, to the best of the author's knowledge, this is the first time this chemical has been identified in the environment.

Lastly, for *m/z* 439.2931, no clear MS^2 spectra could be obtained due to its low intensity. An unequivocal molecular formula could not be reached due to the absence of fragmentation. Thus, this feature remained as *m/z* of interest (level 5).

4. Conclusions

This study presents the largest monitoring of CECs in the groundwater-seawater interface ever performed to-date. It took place in a well characterized Mediterranean coastal aquifer near Barcelona and included wide-scope target analysis for over 2000 chemicals. It resulted in 92 anthropogenic chemical positive identifications spread out over the different zones of the aquifer, including industrial chemicals, pharmaceuticals, biocides, or personal care products. This high number of anthropogenic chemicals indicated the significant influence human activities have on the chemical composition of environmental water at all levels, including barely accessible coastal aquifers. Additionally, these chemicals may reach the marine ecosystem through SGD along with other sea inputs. Hence, 44 chemicals out of the 92 detected in the aquifer, were also found in the sea samples. Nonetheless, their abundance was estimated to be far lower than in the aquifer, in most cases.

Additionally, eight of the identified chemicals, all of them known for their persistent behavior, were proposed as SGD tracers based on its inverse correlation with salinity. PFAS stood out among the selected chemicals, as six members of this family followed this trend, as well as two pharmaceuticals: carbamazepine and topiramate. Non-target analytical strategies were also applied in this study and resulted in the prioritization of three additional features, also candidates for tracing SGD. Among them, one was tentatively identified as 2-(difluoromethylene)− 3,3,4,4,5,5,6,6,7,7,8,8,9,9,10,10,10-heptadecafluoro-decanoic acid. This chemical consisted of a PFAS member, reinforcing the previous results. To the best of our knowledge, this is the first evidence of presence for this perfluorinated chemical in the environment. While recognizing the successful use of those prioritized chemicals as anthropogenic markers during groundwater infiltration, their use as SGD tracers might entail more significant challenges. Hence, the use of PFAS, carbamazepine or topiramate as tracers should be limited to highly contaminated groundwater systems and/or in the context of sea environments with a large proportion of freshwater, such as karstic systems or with a higher resident time in the sea (e.g., semi-closed coastal areas). The determination of naturally occurring substances from the aquifer with very low or even null presence in the sea was among our objectives. The conducted prioritization of the non-target features did not provide natural solid candidates however.

All the provided information enriches the current knowledge on Submarine Groundwater Discharge and the reaction processes occurring at groundwater-seawater interface. While much remains to be done, we conclude that the ability of non-target analyses to identify unsuspected chemicals might contribute to distinguishing the sources of water in coastal aquifers, as well as their organic pollution and degradation processes.

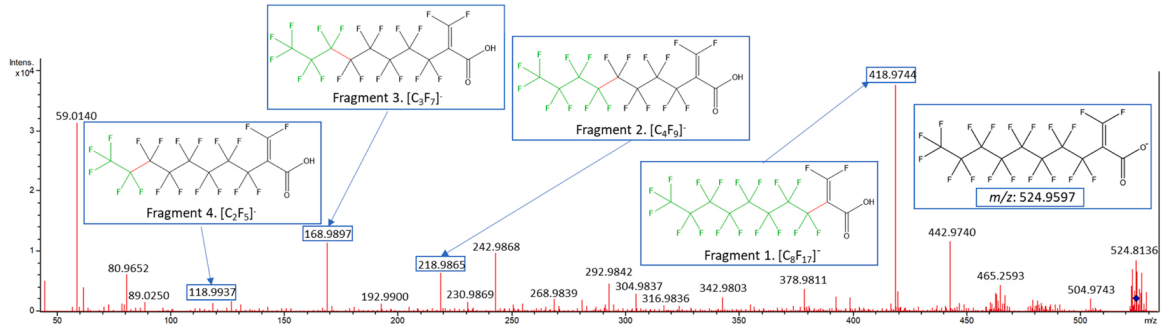

Fig. 6. DDA injection (50 μL injection volume) for the identification of *m/z*: 524.9597.

CRediT authorship contribution statement

D. Gutiérrez-Martín: Formal analysis, Investigation, Data curation, Writing – original draft. **R. Gil-Solsona:** Conceptualization, Methodology, Writing – review & editing, Supervision. **M.W. Saaltink:** Writing - review & editing, Funding acquisition. **V. Rodellas:** Writing– review & editing. **R. López-Serna:** Writing – review & editing. **A. Folch:** Conceptualization, Writing – review & editing, Funding acquisition. **J. Carrera:** Conceptualization, Writing – review & editing, Funding acquisition. **P. Gago-Ferrero:** Conceptualization, Methodology, Writing – review & editing, Project administration, Supervision, Funding acquisition.

Declaration of Competing Interest

The authors declare that they have no known competing financial interests or personal relationships that could have appeared to influence the work reported in this paper.

Data Availability

Data will be made available on request.

Acknowledgments

This work was funded by the project “Mixing and dispersion in the transport of energy and solutes (MEDISTRAES)” coded as PID2019-110212RB-C21 of the Spanish Government (I+D+I Retos Investigación). We acknowledge the contribution of all the members of the MEDISTRAES I, II and III project, from the Groundwater Hydrology Group of the Technical University of Catalonia (UPC) and the Spanish National Research Council (CSIC), the Autonomous University of Barcelona (UAB), the University of Barcelona (UB), the Geosciences Montpellier Laboratory, CNRS and the University of Rennes, for their support during experimental laboratory tests, the Argentona site creation, the setup of the electrodes during piezometer installation and for ensuring site maintenance. IDAEA-CSIC authors would like to express their gratitude to The Spanish Ministry of Science and Innovation through the support received as “Centro de Excelencia Severo Ochoa 2019–2023″. P. Gago-Ferrero acknowledges his Ramón y Cajal fellowship (RYC2019-027913-I) from the AEI-MICI. V. Rodellas acknowledges financial support from the Beatriu de Pinós postdoctoral programme of the Catalan Government (2019-BP-00241).

Appendix A. Supporting information

Supplementary data associated with this article can be found in the online version at doi:10.1016/j.jhazmat.2023.130876.

References

[1] Abarca, E., 2006. Seawater intrusion in complex geological environments. UPC. Technical University of Catalonia.
[2] Adyasari, D., Pratama, M.A., Teguh, N.A., Sabdaningsih, A., Kusumaningtyas, M.A., Dimova, N., 2021. Anthropogenic impact on Indonesian coastal water and ecosystems: current status and future opportunities. In: Mar Pollut Bull, 171. Pergamon, 112689. https://doi.org/10.1016/J.MARPOLBUL.2021.112689.
[3] Alygizakis, N.A., Gago-Ferrero, P., Borova, V.L., Pavlidou, A., Hatzianestis, I., Thomaidis, N.S., 2016. Occurrence and spatial distribution of 158 pharmaceuticals, drugs of abuse and related metabolites in offshore seawater. In: Science of The Total Environment, 541. Elsevier,, pp. 1097–1105. https://doi.org/10.1016/J.SCITOTENV.2015.09.145.
[4] Andrisoa, A., Stieglitz, T.C., Rodellas, V., Raimbault, P., 2019. Primary production in coastal lagoons supported by groundwater discharge and porewater fluxes inferred from nitrogen and carbon isotope signatures. In: Mar Chem, 210. Elsevier B.V,, pp. 48–60. https://doi.org/10.1016/j.marchem.2019.03.003.
[5] Arp, H.P.H., Hale, S.E., 2019. . *REACH: Improvement of guidance and methods for the identification and assessment of PMT/vPvM substances*. Dessau-Roßlau, Germany.
[6] Arpin-Pont, L., Martínez-Bueno, M.J., Gomez, E., Fenet, H., 2016. Occurrence of PPCPs in the marine environment: a review. Environ Sci Pollut Res 23 (6), 4978–4991. https://doi.org/10.1007/s11356-014-3617-x.
[7] Avellan, A., Duarte, A., Rocha-Santos, T., 2022. Organic contaminants in marine sediments and seawater: A review for drawing environmental diagnostics and searching for informative predictors. In: Science of the Total Environment, 808. Elsevier B.V,, 152012. https://doi.org/10.1016/j.scitotenv.2021.152012.
[8] Bakker, M., Miller, A.D., Morgan, L.K., Werner, A.D., 2017. Evaluation of analytic solutions for steady interface flow where the aquifer extends below the sea. J Hydrol 660–664. https://doi.org/10.1016/j.jhydrol.2017.04.009.
[9] Bengtson Nash, S., Rintoul, S.R., Kawaguchi, S., Staniland, I., Van Den Hoff, J., Tierney, M., Bossi, R., 2010. Perfluorinated compounds in the Antarctic region: Ocean circulation provides prolonged protection from distant sources. In: Environmental Pollution, 158. Elsevier Ltd, pp. 2985–2991. https://doi.org/10.1016/j.envpol.2010.05.024.
[10] Brumovský, M., Bečanová, J., Kohoutek, J., Borghini, M., Nizzetto, L., 2017. Contaminants of emerging concern in the open sea waters of the Western Mediterranean. Environ Pollut 229, 976–983. https://doi.org/10.1016/j.envpol.2017.07.082.
[11] Chidichimo, F., De Biase, M., Rizzo, E., Masi, S., Straface, S., 2015. Hydrodynamic parameters estimation from self-potential data in a controlled full scale site. In: J Hydrol (Amst), 522. Elsevier B.V, pp. 572–581. https://doi.org/10.1016/j.jhydrol.2015.01.022.
[12] Clara, M., Strenn, B., Kreuzinger, N., 2004. Carbamazepine as a possible anthropogenic marker in the aquatic environment: Investigations on the behaviour of Carbamazepine in wastewater treatment and during groundwater infiltration. Water Res 38 (4), 947–954. https://doi.org/10.1016/j.watres.2003.10.058.
[13] Diego-Feliu, M., Rodellas, V., Alorda-Kleinglass, A., Saaltink, M., Folch, A., Garcia-Orellana, J., 2022. Extreme precipitation events induce high fluxes of groundwater and associated nutrients to coastal ocean. Hydrol Earth Syst Sci 26 (18), 4619–4635. https://doi.org/10.5194/hess-26-4619-2022.
[14] Diego-Feliu, M., Rodellas, V., Saaltink, M.W., Alorda-Kleinglass, A., Goyetche, T., Martínez-Pérez, L., Folch, A., Garcia-Orellana, J., 2021. New perspectives on the use of 224Ra/228Ra and 222Rn/226Ra activity ratios in groundwater studies. J Hydrol (Amst) January, 596. https://doi.org/10.1016/j.jhydrol.2021.126043.
[15] Dührkop, K., Fleischauer, M., Ludwig, M., Aksenov, A.A., Melnik, A.V., Meusel, M., Dorrestein, P.C., Rousu, J., Böcker, S., 2019. SIRIUS 4: a rapid tool for turning tandem mass spectra into metabolite structure information. In: Nat Methods, 16. Springer, US, pp. 299–302. https://doi.org/10.1038/s41592-019-0344-8.
[16] Duque, C., Calvache, M.L., Pedrera, A., Martín-Rosales, W., López-Chicano, M., 2008. Combined time domain electromagnetic soundings and gravimetry to determine marine intrusion in a detrital coastal aquifer (Southern Spain). J Hydrol (Amst) 349 (3–4), 536–547. https://doi.org/10.1016/j.jhydrol.2007.11.031.
[17] Duque, C., Knee, K.L., Russoniello, C.J., Sherif, M., Abu Risha, U.A., Sturchio, N.C., Michael, H.A., 2019. Hydrogeological processes and near shore spatial variability of radium and radon isotopes for the characterization of submarine groundwater discharge. *J Hydrol (Amst)*, 579 (September): 124192. Elsevier,. https://doi.org/10.1016/j.jhydrol.2019.124192.
[18] EEA. 2016. “Seawater intrusion in coastal aquifers.” Accessed July 6, 2022. ⟨https://www.eea.europa.eu/publications/92–9167-056–1/page010.html⟩.
[19] Falgàs Parra, E., 2007. Hydrogeophysics as a multidisciplinary tool on aquifer appraisal: Focus on AMT capabilities. University of Barcelona, (UB).
[20] Folch, A., del Val, L., Luquot, L., Martínez-Pérez, L., Bellmunt, F., Le Lay, H., Rodellas, V., Ferrer, N., Palacios, A., Fernández, S., Marazuela, M.A., Diego-Feliu, M., Pool, M., Goyetche, T., Ledo, J., Pezard, P., Bour, O., Queralt, P., Marcuello, A., Garcia-Orellana, J., Saaltink, M.W., Vázquez-Suñé, E., Carrera, J., 2020. Combining fiber optic DTS, cross-hole ERT and time-lapse induction logging to characterize and monitor a coastal aquifer (May). In: J Hydrol (Amst), 588. Elsevier,, 125050. https://doi.org/10.1016/j.jhydrol.2020.125050 (May).
[21] Gago-Ferrero, P., Schymanski, E.L., Bletsou, A.A., Aalizadeh, R., Hollender, J., Thomaidis, N.S., 2015. Extended suspect and non-target strategies to characterize emerging polar organic contaminants in raw wastewater with LC-HRMS/MS. Environ Sci Technol 49 (20), 12333–12341. https://doi.org/10.1021/acs.est.5b03454.
[22] Gago-Ferrero, P., Bletsou, A.A., Damalas, D.E., Aalizadeh, R., Alygizakis, N.A., Singer, H.P., Hollender, J., Thomaidis, N.S., 2020. Wide-scope target screening of >2000 emerging contaminants in wastewater samples with UPLC-Q-ToF-HRMS/MS and smart evaluation of its performance through the validation of 195 selected representative analytes (July 2019). In: J Hazard Mater, 387. Elsevier, 121712. https://doi.org/10.1016/j.jhazmat.2019.121712 (July 2019).
[23] Garcia-Orellana, J., Rodellas, V., Tamborski, J., Diego-Feliu, M., van Beek, P., Weinstein, Y., Charette, M., Alorda-Kleinglass, A., Michael, H.A., Stieglitz, T., Scholten, J., 2021. Radium isotopes as submarine groundwater discharge (SGD) tracers: review and recommendations (April). In: Earth Sci Rev, 220. Elsevier B.V,, 103681. https://doi.org/10.1016/j.earscirev.2021.103681 (April).
[24] Gaw, S., Thomas, K.V., Hutchinson, T.H., 2014. “Sources, impacts and trends of pharmaceuticals in the marine and coastal environment.”. Philos Trans R Soc B: Biol Sci.
[25] Goldman, M., Kafri, U., 2007. Hydrogeophysical applications in coastal aquifers. Appl Hydrogeophys 233–254.
[26] González-Gaya, B., Dachs, J., Roscales, J.L., Caballero, G., Jiménez, B., 2014. “Perfluoroalkylated substances in the global tropical and subtropical surface oceans.”. Environ Sci Technol 48 (22), 13076–13084. https://doi.org/10.1021/es503490z.
[27] Goyetche, T., Pool, M., Carrera, J., Luquot, L., 2022. Hydromechanical characterization of tide-induced head fluctuations in coastal aquifers: the role of

delayed yield and minor permeable layers. J Hydrol (Amst). Elsevier B.V, p. 612. https://doi.org/10.1016/j.jhydrol.2022.128128.
[28] Goyetche, T., Luquot, L., Carrera, J., Martínez-Pérez, L., Folch, A., 2022. Identification and quantification of chemical reactions in a coastal aquifer to assess submarine groundwater discharge composition. In: Science of The Total Environment, 838. Elsevier,, 155978. https://doi.org/10.1016/J.SCITOTENV.2022.155978.
[29] Grau-Martínez, A., Folch, A., Torrentó, C., Valhondo, C., Barba, C., Domènech, C., Soler, A., Otero, N., 2018. "Monitoring induced denitrification during managed aquifer recharge in an infiltration pond. J Hydrol (Amst) 561, 123–135. https://doi.org/10.1016/j.jhydrol.2018.03.044.
[30] Guo, Q., Li, H., Boufadel, M.C., Sharifi, Y., 2010. Hydrodynamics in a gravel beach and its impact on the Exxon Valdez oil. J Geophys Res Oceans 115 (12), 1–21. https://doi.org/10.1029/2010JC006169.
[31] Jurado, A., López-Serna, R., Vázquez-Suné, E., Carrera, J., Pujades, E., Petrovic, M., Barceló, D., 2014. Occurrence of carbamazepine and five metabolites in an urban aquifer. Chemosphere 115 (1), 47–53. https://doi.org/10.1016/j.chemosphere.2014.01.014.
[32] Kanwischer, M., Asker, N., Wernersson, A.S., Wirth, M.A., Fisch, K., Dahlgren, E., Osterholz, H., Habedank, F., Naumann, M., Mannio, J., Schulz-Bull, D.E., 2022. Substances of emerging concern in Baltic Sea water: Review on methodological advances for the environmental assessment and proposal for future monitoring. In: Ambio, 51. Springer, Netherlands, pp. 1588–1608. https://doi.org/10.1007/s13280-021-01627-6.
[33] Koussis, A.D., Mazi, K., Riou, F., Destouni, G., 2015. A correction for Dupuit-Forchheimer interface flow models of seawater intrusion in unconfined coastal aquifers. J Hydrol 525, 277–285. https://doi.org/10.1016/j.jhydrol.2015.03.047.
[34] Kurwadkar, S., Dane, J., Kanel, S.R., Nadagouda, M.N., Cawdrey, R.W., Ambade, B., Struckhoff, G.C., Wilkin, R., 2022. Per- and polyfluoroalkyl substances in water and wastewater: a critical review of their global occurrence and distribution. In: Science of the Total Environment, 809. Elsevier B.V,, 151003. https://doi.org/10.1016/j.scitotenv.2021.151003.
[35] Lall, U., L. Josset, and T. Russo. 2020. "A Snapshot of the World's Groundwater Challenges." https://doi.org/10.1146/annurev-environ-102017.
[36] Li, L., Zheng, H., Wang, T., Cai, M., Wang, P., 2018. Perfluoroalkyl acids in surface seawater from the North Pacific to the Arctic Ocean: Contamination, distribution and transportation. In: Environmental Pollution, 238. Elsevier Ltd,, pp. 168–176. https://doi.org/10.1016/j.envpol.2018.03.018.
[37] Liu, Y.S., Ying, G.G., Shareef, A., Kookana, R.S., 2011. Biodegradation of three selected benzotriazoles under aerobic and anaerobic conditions. Water Research 45 (16), 5005–5014. https://doi.org/10.1016/j.watres.2011.07.001.
[38] Llopis-Albert, C., and D. Pulido-Velazquez. 2013. "Discussion about the validity of sharp-interface models to deal with seawater intrusion in coastal aquifers." https://doi.org/10.1002/hyp.9908.
[39] Maréchal, J.C., Wyns, R., Lachassagne, P., Subrahmanyam, K., Touchard, F., 2003. Anisotropie verticale de la perméabilité de l'horizon fissuré des aquifères de socle: Concordance avec la structure géologique des profils d'altération. In: Comptes Rendus - Geoscience, 335. Elsevier Masson SAS, pp. 451–460. https://doi.org/10.1016/S1631-0713(03)00082-8.
[40] Martínez-Pérez, L., Luquot, L., Carrera, J., Marazuela, M.A., Goyetche, T., Pool, M., Palacios, A., Bellmunt, F., Ledo, J., Ferrer, N., del Val, L., Pezard, P.A., García-Orellana, J., Diego-Feliu, M., Rodellas, V., Saaltink, M.W., Vázquez-Suñé, E., Folch, A., 2022. A multidisciplinary approach to characterizing coastal alluvial aquifers to improve understanding of seawater intrusion and submarine groundwater discharge. J Hydrol (Amst) 607 (January), 127510. https://doi.org/10.1016/j.jhydrol.2022.127510.
[41] McKenzie, T., Habel, S., Dulai, H., 2021. Sea-level rise drives wastewater leakage to coastal waters and storm drains. Limnol Oceano Lett 6 (3), 154–163. https://doi.org/10.1002/lol2.10186.
[42] McKenzie, T., Holloway, C., Dulai, H., Tucker, J.P., Sugimoto, R., Nakajima, T., Harada, K., Santos, I.R., 2020. Submarine groundwater discharge: A previously undocumented source of contaminants of emerging concern to the coastal ocean (Sydney, Australia). In: Mar Pollut Bull, 160. Elsevier Ltd, 111519. https://doi.org/10.1016/j.marpolbul.2020.111519.
[43] Menger, F., Ahrens, L., Wiberg, K., Gago-Ferrero, P., 2021. Suspect screening based on market data of polar halogenated micropollutants in river water affected by wastewater. J Hazard Mater. Elsevier, p. 401. https://doi.org/10.1016/j.jhazmat.2020.123377.
[44] Moore, W.S., 2010. The effect of submarine groundwater discharge on the ocean. Ann Rev Mar Sci 2 (1), 59–88. https://doi.org/10.1146/annurev-marine-120308-081019.
[45] Ozler, H.M., 2003. Hydrochemistry and salt-water intrusion in the Van aquifer, east Turkey. Environ Geol 43 (7), 759–775. https://doi.org/10.1007/s00254-002-0690-0.
[46] Palacios, A., José Ledo, J., Linde, N., Luquot, L., Bellmunt, F., Folch, A., Marcuello, A., Queralt, P., Pezard, P.A., Martínez, L., del Val, L., Bosch, D., Carrera, J., 2020. Time-lapse cross-hole electrical resistivity tomography (CHERT) for monitoring seawater intrusion dynamics in a Mediterranean aquifer. Hydrol Earth Syst Sci 24 (4), 2121–2139. https://doi.org/10.5194/hess-24-2121-2020.
[47] Pluskal, T., S. Castillo, A. Villar-Briones, and M. Orešič. 2010. *MZmine 2: Modular framework for processing, visualizing, and analyzing mass spectrometry-based molecular profile data.*
[48] Pool, M., Carrera, J., 2011. A correction factor to account for mixing in Ghyben-Herzberg and critical pumping rate approximations of seawater intrusion in coastal aquifers. Water Resour Res 47 (5). https://doi.org/10.1029/2010WR010256.
[49] Robinson, C., Gibbes, B., Carey, H., Li, L., 2007. Salt-freshwater dynamics in a subterranean estuary over a spring-neap tidal cycle. J Geophys Res 112 (C9), C09007. https://doi.org/10.1029/2006JC003888.
[50] Ruttkies, C., Neumann, S., Posch, S., 2019. Improving MetFrag with statistical learning of fragment annotations. In: BMC Bioinformatics, 20. BMC Bioinformatics, pp. 1–14. https://doi.org/10.1186/s12859-019-2954-7.
[51] Ruttkies, C., Schymanski, E.L., Wolf, S., Hollender, J., Neumann, S., 2016. MetFrag relaunched: Incorporating strategies beyond in silico fragmentation. In: J Cheminform, 8. Springer International Publishing, pp. 1–16. https://doi.org/10.1186/s13321-016-0115-9.
[52] Santos, I.R., Chen, X., Lecher, A.L., Sawyer, A.H., Moosdorf, N., Rodellas, V., Tamborski, J., Cho, H.M., Dimova, N., Sugimoto, R., Bonaglia, S., Li, H., Hajati, M. C., Li, L., 2021. Submarine groundwater discharge impacts on coastal nutrient biogeochemistry. Nat Rev Earth Environ 2 (5), 307–323. https://doi.org/10.1038/s43017-021-00152-0.
[53] Savatier, M., Rocha, C., 2021. Rethinking tracer-based (Ra, Rn, salinity) approaches to estimate point-source submarine groundwater discharge (SGD) into coastal systems. In: J Hydrol (Amst), 598. Elsevier B.V, 126247. https://doi.org/10.1016/j.jhydrol.2021.126247.
[54] Schymanski, E.L., Jeon, J., Gulde, R., Fenner, K., Ruff, M., Singer, H.P., Hollender, J., 2014. Identifying small molecules via high resolution mass spectrometry: Communicating confidence. Environ Sci Technol 48 (4), 2097–2098. https://doi.org/10.1021/es5002105.
[55] Shi, Z.-Q., Liu, Y.-S., Xiong, Q., Cai, W.-W., Ying, G.-G., 2019. Occurrence, toxicity and transformation of six typical benzotriazoles in the environment: A review. The Science of the Total Environment 661, 407–421. https://doi.org/10.1016/j.scitotenv.2019.01.138.
[56] Sims, J.L., Stroski, K.M., Kim, S., Killeen, G., Ehalt, R., Simcik, M.F., Brooks, B.W., 2022. Global occurrence and probabilistic environmental health hazard assessment of per- and polyfluoroalkyl substances (PFASs) in groundwater and surface waters. In: Science of the Total Environment, 816. Elsevier B.V, 151535. https://doi.org/10.1016/j.scitotenv.2021.151535.
[57] Spiteri, C., Slomp, C.P., Tuncay, K., Meile, C., 2008. Modeling biogeochemical processes in subterranean estuaries: Effect of flow dynamics and redox conditions on submarine groundwater discharge of nutrients. Water Resour Res 44 (2). https://doi.org/10.1029/2007WR006071.
[58] Szymczycha, B., Borecka, M., Białk-Bielińska, A., Siedlewicz, G., Pazdro, K., 2020. Submarine groundwater discharge as a source of pharmaceutical and caffeine residues in coastal ecosystem: bay of Puck, southern Baltic Sea case study. Sci Total Environ 713. https://doi.org/10.1016/j.scitotenv.2020.136522.
[59] Tamez-Meléndez, C., Hernández-Antonio, A., Gaona-Zanella, P.C., Ornelas-Soto, N., Mahlknecht, J., 2016. Isotope signatures and hydrochemistry as tools in assessing groundwater occurrence and dynamics in a coastal arid aquifer. Environ Earth Sci 75 (9). https://doi.org/10.1007/s12665-016-5617-2.
[60] Taniguchi, M., Dulai, H., Burnett, K.M., Santos, I.R., Sugimoto, R., Stieglitz, T., Kim, G., Moosdorf, N., Burnett, W.C., 2019. Submarine groundwater discharge: updates on its measurement techniques, geophysical drivers, magnitudes, and effects. Front Environ Sci. Frontiers Media S.A.
[61] Trezzi, G., Garcia-Orellana, J., Rodellas, V., Santos-Echeandia, J., Tovar-Sánchez, A., Garcia-Solsona, E., Masqué, P., 2016. Submarine groundwater discharge: a significant source of dissolved trace metals to the North Western Mediterranean Sea. In: Mar Chem, 186. Elsevier B.V, pp. 90–100. https://doi.org/10.1016/j.marchem.2016.08.004.
[62] U.S. EPA 1993. "Wellhead Protection: A Guide for Small Communities. EPA/625/R-93/002."
[63] U.S. EPA 2022. "Contaminants of Emerging Concern including Pharmaceuticals and Personal Care Products." Accessed August 16, 2022. ⟨https://www.epa.gov/wqc/contaminants-emerging-concern-including-pharmaceuticals-and-personal-care-products⟩.
[64] Vallejos, A., Sola, F., Pulido-Bosch, A., 2015. Processes influencing groundwater level and the freshwater-saltwater interface in a coastal aquifer. Water Resour Manag 29 (3), 679–697. https://doi.org/10.1007/s11269-014-0621-3.
[65] Yu, X., Xin, P., Lu, C., 2019. Seawater intrusion and retreat in tidally-affected unconfined aquifers: laboratory experiments and numerical simulations. In: Adv Water Resour, 132. Elsevier Ltd,. https://doi.org/10.1016/j.advwatres.2019.103393.
[66] Zamrsky, D., Karssenberg, M.E., Cohen, K.M., Bierkens, M.F.P., Oude Essink, G.H. P., 2020. Geological Heterogeneity of Coastal Unconsolidated Groundwater Systems Worldwide and Its Influence on Offshore Fresh Groundwater Occurrence. Front Earth Sci (Lausanne) 7 (January), 1–23. https://doi.org/10.3389/feart.2019.00339.
[67] Zhang, X., Lohmann, R., Sunderland, E.M., 2019. Poly- And Perfluoroalkyl Substances in Seawater and Plankton from the Northwestern Atlantic Margin (research-article). In: Environ Sci Technol, 53. American Chemical Society, pp. 12348–12356. https://doi.org/10.1021/acs.est.9b03230.
[68] Zhou, Y., Sawyer, A.H., David, C.H., Famiglietti, J.S., 2019. Fresh Submarine Groundwater Discharge to the Near-Global Coast. Geophys Res Lett 46 (11), 5855–5863. https://doi.org/10.1029/2019GL082749.